Pressure evolution of the electronic structure of non-centrosymmetric EuRhGe3

Utsumi, Yuki; Batistić, Ivo; Balédent, V.; Shieh, S. R.; Dhami, Naveen Singh; Bednarchuk, O.; Kaczorowski, D.; Ablett, J. M.; Rueff, J. P.

Source / Izvornik: **Electronic Structure, 2021, 3**

Journal article, Published version
Rad u časopisu, Objavljena verzija rada (izdavačev PDF)

https://doi.org/10.1088/2516-1075/ac0c27

Pressure evolution of the electronic structure of non-centrosymmetric $EuRhGe_3$

Electronic Structure

OPEN ACCESS

PAPER

Pressure evolution of the electronic structure of non-centrosymmetric $EuRhGe_3$

Y Utsumi[1,*], I Batistić[2], V Balédent[3], S R Shieh[4], N S Dhami[1], O Bednarchuk[5], D Kaczorowski[5], J M Ablett[6] and J P Rueff[6,7]

[1] Institute of Physics, Bijenička 46, 10000 Zagreb, Croatia
[2] Department of Physics, Faculty of Science, University of Zagreb, Bijenička 32, 10000 Zagreb, Croatia
[3] Université Paris-Saclay, CNRS, Laboratoire de Physique des Solides, 91405 Orsay, France
[4] Department of Earth Sciences, Department of Physics and Astronomy, University of Western Ontario, London, Ontario, N6A 5B7, Canada
[5] Institute of Low Temperature and Structure Research, Polish Academy of Sciences, Okólna 2, 50-422 Wrocław, Poland
[6] Synchrotron SOLEIL, L'Orme des Merisiers, BP 48, St Aubin, 91192 Gif-sur-Yvette, France
[7] Laboratoire de Chimie Physique-Matière et Rayonnement, Sorbonne Université, CNRS, 75005 Paris, France
[*] Author to whom any correspondence should be addressed.

E-mail: yutsumi@ifs.hr

Keywords: Eu valence, pressure, x-ray absorption, electronic structure

RECEIVED
1 February 2021

REVISED
2 June 2021

ACCEPTED FOR PUBLICATION
17 June 2021

PUBLISHED
15 July 2021

Abstract

Among europium compounds, pressure induced valence transitions and/or intermediate valence states are often observed. In such systems, applying pressure of several GPa can drive a Eu valence from divalent to almost trivalent. Non-centrosymmetric $EuRhGe_3$ possesses magnetic Eu^{2+} ions and exhibits antiferromagnetic ordering at ∼11 K at ambient pressure. Pressure resistant magnetic ordering and stable divalent Eu state have been reported in $EuRhGe_3$. Here, we study the pressure evolution of the Eu valence of $EuRhGe_3$ by high resolution x-ray absorption spectroscopy using the partial fluorescence yield method. Our study reveals a successive increase of the Eu valence with increasing pressure without any valence transition. The obtained mean Eu valence approaches ∼2.4 around 40 GPa at 300 K. The experimental data are also analyzed by a full multiplet configuration interaction calculation based on the single impurity Anderson model. The analysis reveals a decrease of the Eu 4*f* orbital occupation by applying pressure. Pressure evolution of the electronic structure studied by density functional theory suggests that the Rh ions have little contribution to the pressure evolution of the Eu valence, while it implies an active involvement of the Ge ions.

1. Introduction

Since the discovery of the first heavy fermion superconductor $CeCu_2Si_2$ [1], over 30 systems have been revealed to exhibit unconventional *f*-electron superconductivity [2]. Most of them are among the Ce- and U-compounds, and their phase diagrams are often described using the Doniach model [3]. The ground state is characterized by a competition between the Kondo effect and the Ruderman–Kittel–Kasuya–Yosida (RKKY) interactions that both originate from the interplay of localized *f* electrons and itinerant conduction electrons. The Kondo effect quenches the magnetic moments, while the RKKY interaction stabilizes the magnetic ordering. Usually, the superconductivity emerges in the vicinity of the magnetic quantum critical point (QCP). Recently, heavy fermion superconductors were discovered among the compounds without inversion symmetry in their crystal structures. They have been attracting considerable attention due to the possible coexistence of spin- singlet and-triplet Cooper pairing channels initiated by anti-symmetric spin–orbit coupling and strong correlations [4, 5]. Except the previously discovered $CePt_3Si$ [6], the superconductivity in the noncentrosymmetric compounds tends to develop under pressure [7–10]. The antiferromagnetic $CeTX_3$ (T = Co, Rh, Ir; X = Si, Ge) series possess the $BaNiSn_3$-type structure ($I4mm$) which is similar to the $ThCr_2Si_2$-type structure,

though without centrosymmetry. Applying pressure continuously decreases the magnetic ordering temperature (T_N) and the superconductivity appears near QCP or coexists with strongly suppressed magnetic ordering [7–10]. Similarly to the $BaNiSn_3$-type structure, a series of Eu-compounds $EuTX_3$ (T: d-electron transition metal, X = Si, Ge) has been discovered. Yet, an emergence of pressure induced superconductivity in those materials has not been reported.

Eu-compounds, in general, tend to exhibit pressure-temperature phase diagrams distinctly different from those of Ce-compounds. Most of the reported Eu-phases favour a Eu^{2+} ($4f^7$, $J = 7/2$) valence state at ambient pressure with an antiferromagnetic ground state. However, the energy difference between Eu^{2+} and the non-magnetic Eu^{3+} ($4f^6$, $J = 0$) valence states is not so large [11] and is reachable by applying external pressure or chemical substitution. A typical first-order valence transition induced by pressure or chemical substitution can be found among a series of Eu-compounds with the $ThCr_2Si_2$-type crystal structure [12]. Applying pressure on such compounds increases T_N, then a sudden disappearance of magnetic moments and a valence crossover happen at a critical pressure. In contrast, an atypical pressure response has been reported in $Eu_2Ni_3Ge_5$ and $EuRhSi_3$ [13–15]. Both compounds are antiferromagnets with almost divalent Eu ions at ambient pressure. Applying pressure causes an increase of T_N up to 5–7 GPa, yet at higher pressure T_N smoothly decreases in a manner compatible with the Doniach-type phase diagram [13, 15]. Pressure dependent resistivity measurements suggested a continuous change of the Eu valence without a first-order valence transition [15]. This behavior opens a possibility of the occurrence in these materials of QCP as well as the emergence of superconductivity in its vicinity.

$EuRhGe_3$ is isostructural to $EuRhSi_3$ possessing the $BaNiSn_3$-type crystal structure. The Eu valence is expected to be almost divalent at ambient pressure, and antiferromagnetic ordering emerges at ∼11 K with the magnetic moments aligned perpendicular to the c-axis [16–18]. A pressure dependent electrical resistance measurement of $EuRhGe_3$ was reported only up to 8 GPa where T_N showed a monotonous increase [19]. Considering the high critical pressure $P_c < 30$ GPa predicted for $EuRhSi_3$ [15], the suppression of the magnetic ordering and reaching a potential QCP in $EuRhGe_3$ might also require similarly high pressure. However, transport measurements under such high pressures are challenging and hence no such experimental results have been reported to date.

Since the Eu valence state in Eu-compounds is related to their magnetic behaviors, studying pressure evolution of the Eu valence provides complementary information to understand the pressure phase diagram. We performed high resolution x-ray absorption spectroscopy at the Eu L_3 edge as a function of pressure and studied the change of the Eu valence in $EuRhGe_3$. In combination with density functional theory (DFT), we analyzed the pressure evolution of the electronic structure of $EuRhGe_3$. The experimental results show a continuous increase of the Eu valence by applying pressure without a first-order valence/phase transition. The obtained mean Eu valence (v) reaches $v \sim 2.4$ at 40 GPa. The Eu L_3 XAS structures and the pressure evolutions are also analyzed by a full multiplet configuration interaction calculation based on the single impurity Anderson model (SIAM). The analysis reveals a decrease of the Eu 4f orbital occupation by applying pressure. The results of the DFT calculation suggest that a rather small contribution from the Rh ions to the pressure evolution of the Eu valence, while that implies an active involvement of the Ge ions. Applying pressure slightly changes the Eu 5d band structure, though the effect plays a minor role in the pressure variation of the Eu L_3 XAS structures.

2. Experimental

High resolution partial fluorescence yield x-ray absorption spectroscopy (PFY-XAS) measurements were performed at the GALAXIES beamline [20–22] of the SOLEIL synchrotron. A Ge (333) analyzer crystal with a Bragg angle 77° was used to select the Eu $L_{\alpha 1}$ emission line (5846 eV) and the incident energy was swept across the Eu L_3-edge using a Si (111) double crystal monochromator. The intensity of the emitted photons was recorded by using a silicon drift detector. The PFY-XAS spectra were measured at 90° scattering angle with incident and outgoing photons passing through a Be gasket. The sample, analyzer and detector were all situated in a vertical Rowland circle geometry.

$EuRhGe_3$ single crystal was grown by the metal-flux method and characterized by x-ray diffraction, magnetic susceptibility and electrical resistivity measurements [16]. The sample was loaded inside a symmetrical diamond anvil cell using Be gasket with Ne gas as pressure transmitting medium and ruby spheres used to measure pressure by ruby fluorescence method [23]. The applied pressure was measured before and after the measurement at each pressure points and averaged.

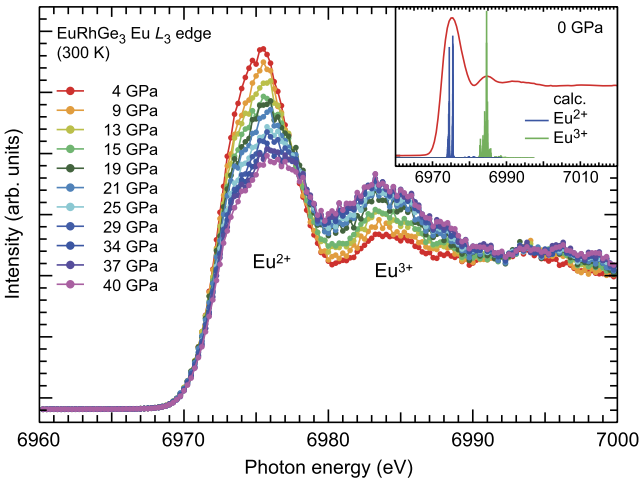

Figure 1. Pressure dependent Eu L_3 PFY-XAS spectra of $EuRhGe_3$ measured at 300 K. Inset shows the spectrum at ambient pressure and the results of atomic multiplet calculations of Eu^{2+} (blue) and Eu^{3+} (green) obtained by using the XTLS 9.01 code [24]. The electrostatic and exchange parameters were obtained by using Cowan's atomic Hartree–Fock program with relativistic corrections [25]. The exchange parameters were scaled down to 86% of their Hartree–Fock values to obtain a good agreement with the experimental spectra.

3. Results and discussion

Figure 1 shows the pressure dependent Eu L_3 PFY-XAS spectra of $EuRhGe_3$ measured at 300 K. The inset of figure 1 shows the Eu L_3 spectrum at ambient pressure and the results of atomic multiplet calculations of the Eu L_3 XAS spectra with Eu f^7 (Eu^{2+}) and $4f^6$ (Eu^{3+}) electron configurations obtained by using the XTLS 9.01 code [24]. The PFY-XAS spectra were observed by scanning the incident x-ray energy through the Eu L_3 absorption edge and recording scattered intensity at the Eu $L_{\alpha 1}$ fluorescence energy. Although the PFY-XAS spectra resemble a standard XAS spectrum, the spectral shape is sharper due to the absence of a deep $2p$ core hole in the final state. The Eu L_3 PFY-XAS spectra exhibit a prominent peak at 6975 eV and a broad peak centered at 6984 eV corresponding to Eu^{2+} ($2p^6 4f^7 \rightarrow 2p^5 4f^7 + \epsilon d(\epsilon s) \rightarrow 2p^6 3d^9 4f^7$) and Eu^{3+} ($2p^6 4f^6 \rightarrow 2p^5 4f^6 + \epsilon d(\epsilon s) \rightarrow 2p^6 3d^9 4f^6$) components, respectively. Although the transition process does not directly include the $4f$ states, the Eu^{2+} and Eu^{3+} peaks in the Eu L_3 PFY-XAS spectra are well separated and sensitive to the change of the Eu valence due to strong Coulomb interaction between the $3d$ core hole and the final state $4f$ electron. A broad satellite peak is present around 20 eV above the main line. This feature has been reported for other Eu compounds and considered to be related to the intralayer and interlayer electronic states in a layered system [26]. With an increase in pressure, the intensity of the Eu^{2+} peak decreases, while that of the Eu^{3+} increases. The change in the relative intensity between Eu^{2+} and Eu^{3+} peaks indicates a variation of the Eu valence and formation of an intermediate valence state under high pressure.

In order to obtain the mean Eu valence, we performed a fitting analysis on the Eu L_3 PFY-XAS spectra using three Gaussian functions corresponding to Eu^{2+}, Eu^{3+}, and the satellite peaks, and two arctangent backgrounds for each of the Eu^{2+} and Eu^{3+} components (see figure 2(a)). We did not take into account quadrupolar $2p \rightarrow 4f$ excited states which can be present in the pre-edge region. We estimated the Eu mean valence using the formula $v = 2 + I_{3+}/(I_{2+} + I_{3+})$. Here I_{2+} and I_{3+} denote the integrated spectral intensities of the Eu^{2+} and Eu^{3+} peaks extracted from the fitting analysis. Note that the intensity of the satellite peak was not included in the Eu valence estimation. The obtained v is plotted in figure 2(b) as a function of pressure. The Eu valence obtained at ambient pressure is 2.13 ± 0.02 which is similar to the value obtained in the earlier photoelectron spectroscopy (PES) experiment [27]. With increasing pressure up to 20 GPa, v linearly increases, and at higher pressures shows a tendency towards saturation. The latter feature may arise due to a change in compressibility of $EuRhGe_3$ since no structural transition driven by pressure was observed at room temperature. Below 10 GPa, the mean Eu valence remains in the range of $2.0 \leqslant v \leqslant 2.2$ where the magnetic ordering and the intermediate valence state can coexist [28]. This finding is also consistent with the reported pressure dependent electrical resistivity data that indicated the presence of Eu^{2+} ions and preserved antiferromagnetic ordering up to 8 GPa [19]. The Eu mean valence reaches $v \sim 2.4$ around 40 GPa. No valence/phase transitions was found in the entire pressure range investigated. A stable Eu^{2+} valence state is rather uncommon for Eu-compounds. For the most intensively studied ternaries with the $ThCr_2Si_2$-type structure, a valence transition from Eu^{2+} to almost Eu^{3+}, induced by pressure or substitution by smaller atoms usually occurs [12]. For example, antiferromagnet $EuRh_2Si_2$ has been reported to undergo a valence transition by applying pressure,

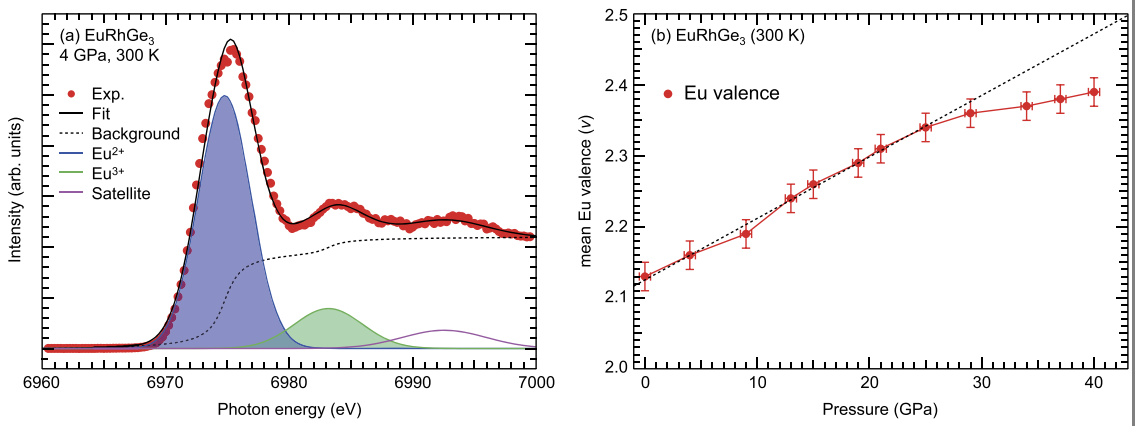

Figure 2. (a) An example of fitting the Eu L_3 PFY-XAS spectrum by using three Gaussian functions and two arctangent backgrounds. Peak widths, full width at half maximum (FWHM), of Eu^{2+} and Eu^{3+} valence states are slightly changed in the energy ranges of 5–6 eV and 6.5–7.5 eV, respectively, and that of the satellite is fixed at 8 eV. (b) The mean Eu valence as a function of pressure. The dashed line marks a linearity of the pressure dependence of v in the pressure range 0–25 GPa.

with a corresponding v changes from ∼2.2 at ambient pressure to ∼ +2.9 around 8 GPa at 300 K [29]. In the case of $EuNi_2Si_2$, a pressure dependent ^{151}Eu-Mössbauer isomer shift indicated the change of Eu valence from almost Eu^{2+} at ambient pressure to Eu^{3+} around 8 GPa at 300 K without a structural transition [30]. A rather stable Eu^{2+} state with pressure was reported in the antiferromagnetic $EuFe_2As_2$. The mean Eu valence obtained by means of Eu L_3 XAS continuously changes from Eu^{2+} at ambient pressure to $v \sim 2.4$ around 25 GPa at 300 K without a first order valence transition [31].

In order to study the pressure induced change in the electronic structure of $EuRhGe_3$, we performed band structure calculations using the QUANTUM ESPRESSO software [32]. In our DFT calculations, we have used pseudopotentials from pslibrary 1.0.0 [33] and the Perdew–Burke–Ernzerhof exchange-correlation functional for solids [34, 35]. Brillouin zone integration was performed on a 12 ×12× 6 k-points mesh without offset and the Marzari–Vanderbilt Fermi surface smearing function [36]. The Hubbard interaction was taken into account by using a simplified scheme of DFT + U [37]. The Hubbard interaction U for Eu was assumed to be 3.8 eV in order to match the Eu 4f peak position observed in the PES experiment [27]. The U value was fixed to a constant throughout the whole pressure region. Figure 3 shows the simulated partial DOS that mainly contribute to the valence band and their sum at 0, 20, and 43 GPa. The simulated DOS at ambient pressure is consistent with the previous result [27]. The Eu 4f orbitals are almost half occupied and the 4f DOS is localized at −1 eV. The majority of Eu 5d DOS is unoccupied and centered at ∼5 eV (see also figure 4(a)), while the occupied part is widely extended in the valence band. The occupied Rh 4d and Ge 4p DOS appear in the same energy range, from the Fermi level (E_F) to −6 eV. The occupied Ge 4s DOS appears from −7 to −12 eV (not shown here) and its unoccupied part overlaps with the unoccupied Eu 5d DOS. With an increase in pressure, the centre of the Rh 4d DOS slightly shifts away from E_F. The total DOS at 0 GPa has a quasi-gap like low-DOS region located ∼ 1.5 eV above E_F, though it completely disappears at 43 GPa. Since the increase (decrease) of Eu^{3+} (Eu^{2+}) peak intensity is observed in the Eu L_3 XAS spectra by applying pressure, a decrease of the Eu 4f orbital occupation is expected. However, the amount of charge transfer of Eu 4f estimated by using Lowdin charge analysis [38] shows a little decrease with increasing pressure, achieving only $\Delta n \sim 0.06$ at 43 GPa. The largest changes are expected in the Eu 5d and Ge 4s orbitals. In spite of the pressure variation of the Rh 4d band structure, an increase of Rh 4d charge is estimated to be below $\Delta n \sim 0.05$ at 43 GPa, and the total charge on the Rh ions is conserved. This indicates little contribution of Rh ions to the pressure evolution of the Eu valence. We have also simulated the pressure evolution of the electronic structure with Hubbard interaction U values for Eu 4f and Rh 4d obtained by an *ab initio* approach [37, 39–43]. Although the energies of the Eu 4f and Rh 4d DOS vary depending on the calculation parameters, the tendency of pressure variation of the electronic structure does not depend on the U values. The results of the DFT calculation can be interpreted that the observed pressure evolution of the Eu L_3 XAS structures derives from the pressure variation of the Eu 5d band structure. According to our Lowdin charge analysis, a charge transfer from Ge 4s to the Eu 5d orbitals under pressure is expected. However, this contradicts to the experimentally obtained change of the Eu valence. The contradictory result might be arising from the analytical method. The Lowdin charge analysis [38] is based on the projection of extended states onto atomic orbitals. When the atomic orbitals have extended radial distribution functions, such as Eu 5d and Ge 4s, the interstitial electrons are possibly included in the atomic orbitals.

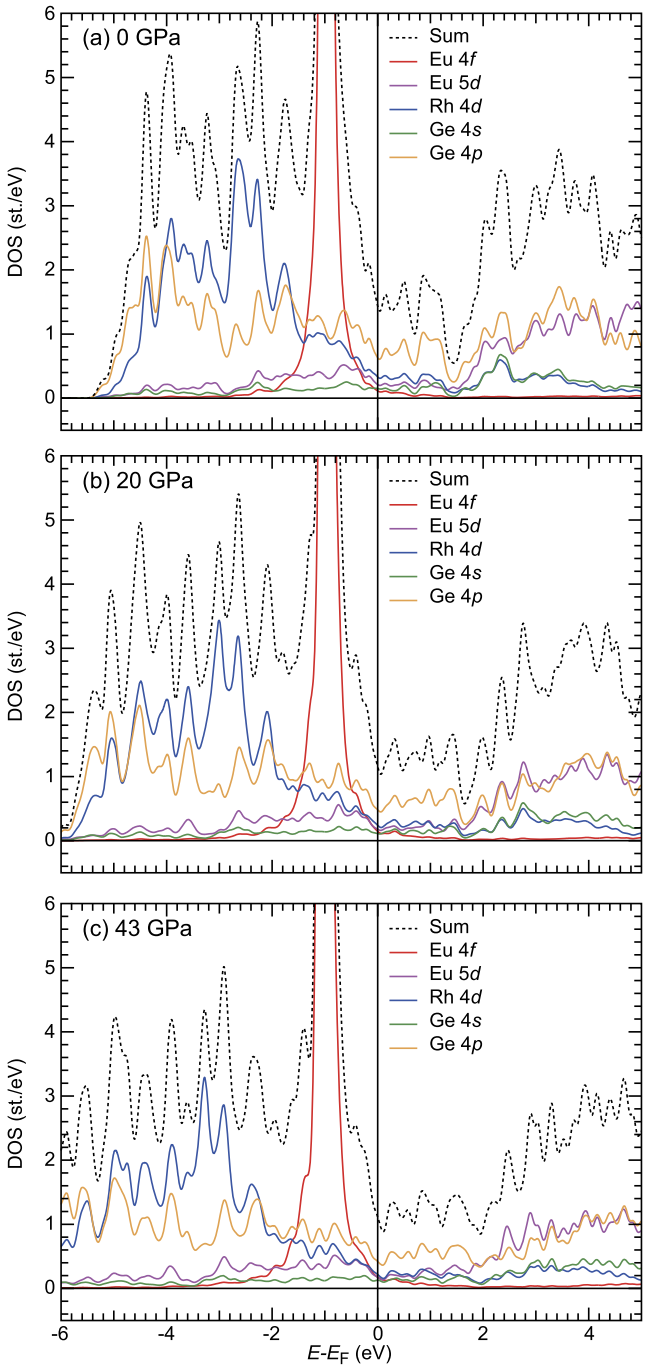

Figure 3. Total and partial density of states (DOS) calculated for $EuRhGe_3$ by DFT + U ($U = 3.8$ eV) at (a) 0 GPa, (b) 20 GPa, and (c) 43 GPa. In $EuRhGe_3$, Ge atoms occupy two different crystallographic sites [16]. Here, the PDOS of all Ge atoms are plotted together.

Since the Eu L_3 spectrum reflects the transition from $2p$ to $5d$ states, the spectral change can be induced not only by the change of the Eu $4f$ orbital occupation but also by that of the Eu $5d$ orbital occupation. An increase of the Eu $5d$ orbital occupation corresponds to a decrease of unoccupied Eu $5d$ states which leads to decrease of the Eu L_3 spectral intensities. Such case has been reported in the pressure evolution of elemental Eu, which is a divalent antiferromagnet at ambient pressure [44]. Applying pressure was expected to lead to trivalent Eu and a weak Van Vleck paramagnetism that can be associated with superconductivity. Indeed, pressure induced superconductivity below $T_c \sim 1.8$ K was discovered to emerge under extremely high pressure ~80 GPa [45]. A pressure dependent Eu L_3 XAS experiment has also reported an intermediate valence under pressure, although the Eu valence did not become fully trivalent state [46]. Notably, T_c found for pressurized Eu was much lower than the critical temperatures established for other superconducting lanthanides [47]. Recently, Bi *et al* revealed that the pressure evolution of Eu L_3 XAS spectra was driven by a change in the Eu $5d$ orbital occupation and the Eu $4f^7$ magnetic moments retained up to 119 GPa [44, 48]. The magnetic

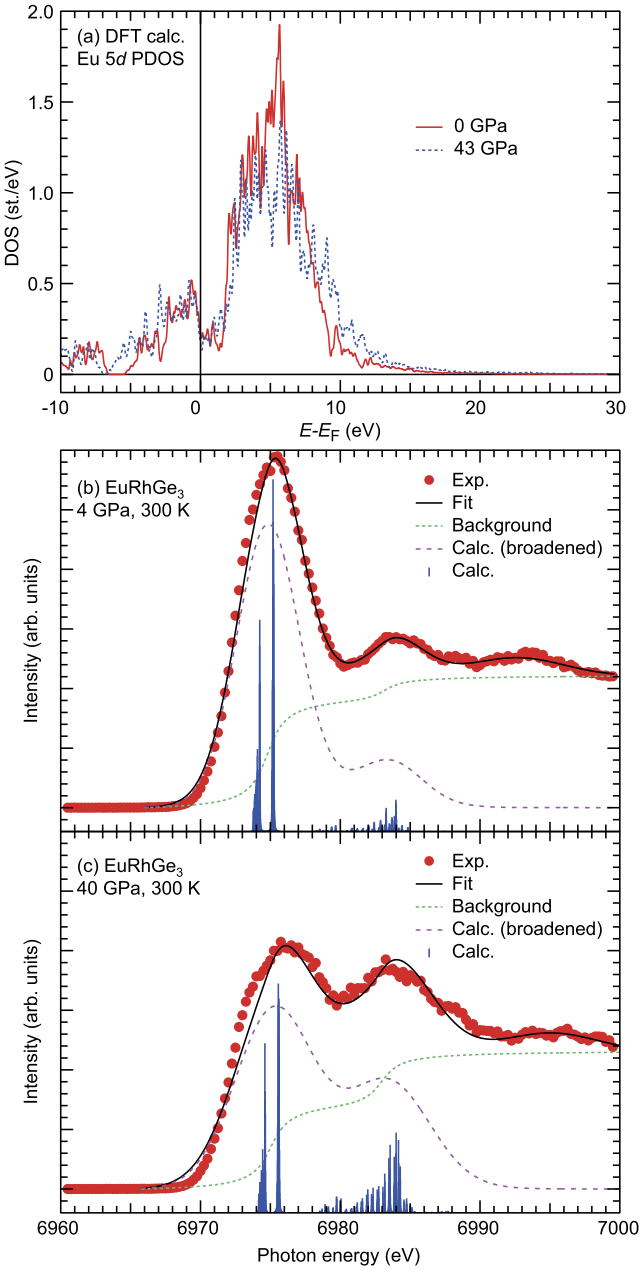

Figure 4. (a) The calculated Eu 5*d* PDOS of $EuRhGe_3$ by DFT + U ($U = 3.8$ eV) with a wide energy range. The solid red and dashed blue lines represent the PDOS at ambient pressure and 43 GPa, respectively. The calculated Eu L_3 XAS structures of (b) 4 GPa and (c) 40 GPa by the full multiplet configuration interaction based on the SIAM. The vertical bars and dashed purple line correspond to the calculated multiplet structures and the ones convoluted with a Gaussian function (FWHM = 5.1 and 6.4 eV for 4 and 40 GPa, respectively). The experimental spectra are fitted by the calculated spectrum, two arctangent backgrounds, and a Gaussian function (FWHM = 8.0 eV) representing the satellite peak.

ordering was reported to remain at high pressures, up to about 80 GPa, where the magnetic fluctuations driven unconventional superconductivity was found to emerge [44, 48, 49]. In order to clarify the effect of the Eu 5*d* band structure on the Eu L_3 XAS structures, we show the calculated Eu 5*d* PDOS at ambient pressure and 43 GPa with a wide energy range in figure 4(a). The unoccupied Eu 5*d* PDOS is centered at ∼5 eV. There are no two peak structures corresponding to the Eu L_3 XAS structures. Applying pressure slightly modifies the Eu 5*d* band structure, though such a small change is unlikely to cause the large pressure variation of the Eu L_3 XAS structures. It is worth to mention an earlier study about the effect of 5*d* band structure on the L_3 XAS structure. The origin of the Ce L_3 XAS structure had been discussed whether it was due to the Ce 5*d* band structure or different valence states of Ce ions. By using the SIAM analysis, Kotani *et al* revealed that the L_3 XAS structure derived from different core-hole potential effect in XAS final state between Ce^{3+} (f^1) and Ce^{4+} (f^0), while the Ce 5*d* band structure had rather a minor effect [50]. In order to investigate the origin of Eu L_3 XAS structure, we also performed a full multiplet configuration interaction calculation based on the SIAM by using XTLS 9.01 code [24]. The electrostatic and exchange parameters were obtained by using Cowan's Hartree–Fock program

Table 1. The parameters used in the full multiplet configuration interaction based on the SIAM calculation for each pressure and the obtained Eu 4*f* electron occupation (n_f).

Pressure (GPa)	U_{ff} (eV)	U_{cf} (eV)	Δ (eV)	U_{fd} (eV)	V_{cf} (eV)	n_f
0	6.5	10.5	1.26	2.5	0.26	6.86
4	6.5	10.5	1.33	3.0	0.27	6.83
9	6.5	10.5	1.34	3.0	0.28	6.82
13	6.5	10.5	1.38	3.0	0.32	6.77
15	6.5	10.5	1.42	3.0	0.32	6.75
19	6.5	10.5	1.46	3.0	0.34	6.71
21	6.5	10.5	1.50	3.0	0.34	6.69
25	6.5	10.5	1.54	3.0	0.34	6.67
29	6.5	10.5	1.57	3.0	0.34	6.65
34	6.5	10.5	1.60	3.0	0.34	6.63
37	6.5	10.5	1.62	3.0	0.34	6.62
40	6.5	10.5	1.64	3.0	0.34	6.61

The values of the *F* and *G* Slater integrals and the spin–orbit interaction (ζ) used for the calculations were obtained by Cowan's atomic Hartree–Fock (HF) program [25]. The obtained HF values are reduced to 86% to obtain a good agreement with the experimental spectra. The parameters of the $4f^6$ and $4f^7\underline{L}$ configurations in the simulations of L_3 XAS spectra are: $(F^2_{4f4f}, F^4_{4f4f}, F^6_{4f4f}, \zeta_{4f}) = (12.168, 7.637, 5.495, 0.175)$ and $(F^2_{4f4f}, F^4_{4f4f}, F^6_{4f4f}, \zeta_{4f}) = (11.229, 7.004, 5.495, 0.160)$, respectively. The parameters of $2p^54f^65d^1$ configuration are: $(F^2_{4f4f}, F^4_{4f4f}, F^6_{4f4f}, \zeta_{4f}) = (13.376, 8.435, 6.081, 0.216)$, $(F^2_{2p4f}, G^2_{2p4f}, G^4_{2p4f}, \zeta_{2p}) = (1.730, 0.181, 0.117, 445.090)$, $(F^2_{4f5d}, F^4_{4f5d}, G^1_{4f5d}, G^3_{4f5d}, G^5_{4f5d}, \zeta_{5d}) = (3.237, 1.559, 1.324, 1.132, 0.879, 0.175)$, and $(F^2_{2p5d}, G^1_{2p5d}, G^3_{2p5d}) = (0.480, 0.410, 0.242)$, and those of $2p^54f^7\underline{L}5d^1$ configuration are: $(F^2_{4f4f}, F^4_{4f4f}, F^6_{4f4f}, \zeta_{4f}) = (12.582, 7.896, 5.682, 0.201)$, $(F^2_{2p4f}, G^2_{2p4f}, G^4_{2p4f}, \zeta_{2p}) = (1.617, 0.168, 0.108, 445.139)$, $(F^2_{4f5d}, F^4_{4f5d}, G^1_{4f5d}, G^3_{4f5d}, G^5_{4f5d}, \zeta_{5d}) = (2.691, 1.276, 1.196, 0.965, 0.734, 0.124)$, and $(F^2_{2p5d}, G^1_{2p5d}, G^3_{2p5d}) = (0.345, 0.291, 0.172)$.

with relativistic corrections [25]. The exchange parameters were scaled down to 86% of their Hartree–Fock values to obtain a good agreement with the experimental spectra. The ground state and final states of XAS spectrum are described by a linear combination of the electron configurations of $4f^6$ and $4f^7\underline{L}$, and $2p^54f^65d^1$ and $2p^54f^7\underline{L}5d^1$, where $\underline{L}$ denotes a hole in the conduction band below the Fermi energy. A mixing of $4f^6$ and $4f^7\underline{L}$ states due to the hybridization between 4*f* and conduction bands (*c*–*f* hybridization) is described as V_{cf}. The charge transfer energy Δ is defined as $E(4f^7\underline{L}) - E(4f^6)$, where $E(4f^6)$ and $E(4f^7\underline{L})$ are average energies of $4f^6$ and $4f^7\underline{L}$ configurations, respectively. Here, V_{cf} and Δ are adjustable parameters to reproduce the pressure evolution of the Eu L_3 XAS spectrum. The on-site Coulomb interactions between 4*f* electrons (U_{ff}), a 2*p* core-hole and a 4*f* electron (U_{fc}), and 4*f* and 5*d* electrons (U_{fd}) used for the calculation are taken from reference [51]. Here, the Eu 5*d* is treated as a core-level like state, therefore the change of unoccupied 5*d* DOS is not considered in the calculation. The parameters used for the calculation and the obtained number of 4*f* electrons are listed in the table 1. The calculated L_3 XAS structures of 4 and 40 GPa are shown in figures 4(b) and (c), respectively, with the experimental spectra. The calculated structures of 4 GPa exhibit prominent features around 6975 eV and small features at $\sim$ 6984 eV that correspond to the multiplet structures of Eu^{2+} and Eu^{3+}, respectively. The pressure evolution of the L_3 XAS spectra is simulated by changing the values of Δ and V_{cf}. A relationship between the unit cell volume and Δ has been reported in $EuNi_2(Si_{1-x}Ge_x)_2$ [52]. A decrease of the unit cell volume resulted in the increase of Δ, as well as V_{cf}. Since applying hydrostatic pressure reduces the unit cell volume of $EuRhGe_3$, the Eu L_3 XAS spectrum of 40 GPa is calculated by increasing the values of Δ and V_{cf}. The calculated result of 40 GPa in figure 4(c) shows a relative increase of the Eu^{3+} intensity compared to that of the Eu^{2+}. By using the calculated structures convoluted with a Gaussian function, we fit the experimental spectra with two arctangent backgrounds and a Gaussian function (FWHM = 8.0 eV) representing the satellite peak. The analysis shows that the Eu L_3 XAS structures actually derive from the $4f^7$ (Eu^{2+}) and $4f^6$ (Eu^{3+}) configurations, and the pressure evolution of the Eu L_3 XAS structures reflects the variation of the 4*f* electron occupation. While the pressure change of the Eu 5*d* band structure plays a minor role in the pressure evolution of the Eu L_3 XAS structures.

4. Conclusion

We performed PFY-XAS measurements on $EuRhGe_3$ as a function of pressure. The Eu L_3 PFY-XAS spectrum shows the dominant Eu^{2+} state at ambient pressure that is consistent with the earlier PES experiment [27]. With increasing pressure, the intensity of the Eu^{2+} peak decreases while that of the Eu^{3+} increases developing

the intermediate valence state. The obtained mean Eu valence increases linearly up to 25 GPa, and exhibits a smaller change at higher pressures. Around 40 GPa, the mean Eu valence reaches ~ 2.4. Within the experimental pressure range, we did not observe any pressure induced first order valence transition. The pressure evolution of the electronic structure was studied by DFT calculation. The result suggests that the Rh ions have little contribution to the pressure evolution of the Eu valence, while it implies an active involvement of the Ge ions. We also analyzed the Eu L_3 XAS spectra by the full multiplet configuration interaction calculation based on the SIAM. The results confirm that the Eu L_3 XAS structure actually derived from the f^7 (Eu^{2+}) and f^6 (Eu^{3+}) configurations. The study reveals that the pressure evolution of the Eu L_3 XAS structures reflects the decrease of the Eu 4*f* electron occupation by applying pressure. Although the pressure variation of the Eu 5*d* band structure is predicted by the DFT calculations, the effect plays a minor role in the pressure evolution of the Eu L_3 XAS structures. Our study suggests that the magnetic moments of Eu $4f^7$ in $EuRhGe_3$ are likely preserved under high pressure, at least up to $\sim$10 GPa. To suppress the antiferromagnetic ordering towards hypothetical quantum phase transition, possibly associated with the emergence of unconventional superconductivity, pressures higher than 10 GPa are recommended to apply for transport measurements.

Acknowledgments

We would like to thank Dominique Prieur for his skillful technical assistance. YU thanks Osor Barišić and Kojiro Mimura for helpful discussions. The PFY-XAS experiment was performed under the approval of GALAXIES beamline station (proposal No. 20170905). This work has been supported in part by the Croatian Science Foundation under the project number IP-2016-06-7258. The research leading to this result has been supported by the project CALIPSOplus under the Grant Agreement 730872 from the EU Framework Programme for Research and Innovation HORIZON 2020.

Data availability statement

The data that support the findings of this study are available upon reasonable request from the authors.

ORCID iDs

Y Utsumi https://orcid.org/0000-0003-4062-2421

References

[1] Steglich F, Aarts J, Bredl C D, Lieke W, Meschede D, Franz W and Schäfer H 1979 *Phys. Rev. Lett.* **43** 1892–6
[2] Pfleiderer C 2009 *Rev. Mod. Phys.* **81** 1551–624
[3] Doniach S 1977 *Physica B+C* **91** 231–4
[4] Takimoto T 2008 *J. Phys. Soc. Japan* **77** 113706
[5] Takimoto T and Thalmeier P 2009 *J. Phys. Soc. Japan* **78** 103703
[6] Bauer E *et al* 2004 *Phys. Rev. Lett.* **92** 027003
[7] Kimura N, Ito K, Saitoh K, Umeda Y, Aoki H and Terashima T 2005 *Phys. Rev. Lett.* **95** 247004
[8] Sugitani I *et al* 2006 *J. Phys. Soc. Japan* **75** 043703
[9] Settai R, Sugitani I, Okuda Y, Thamizhavel A, Nakashima M, Onuki Y and Harima H 2007 *J. Magn. Magn. Mater.* **310** 844–6
[10] Honda F, Bonalde I, Yoshiuchi S, Hirose Y, Nakamura T, Shimizu K, Settai R and Onuki Y 2010 *Phys.* C **470** S543–4
[11] Bauminger E R, Froindlich D, Nowik I, Ofer S, Felner I and Mayer I 1973 *Phys. Rev. Lett.* **30** 1053–6
[12] Onuki Y *et al* 2017 *Phil. Mag.* **97** 3399–414
[13] Nakamura A *et al* 2015 *J. Phys. Soc. Japan* **84** 053701
[14] Muthu S E, Braithwaite D, Salce B, Nakamura A, Hedo M, Nakama T and Onuki Y 2016 *J. Phys. Soc. Japan* **85** 094603
[15] Nakashima M *et al* 2017 *J. Phys. Soc. Japan* **86** 034708
[16] Bednarchuk O, Gagor A and Kaczorowski D 2015 *J. Alloys Compd.* **622** 432–9
[17] Bednarchuk O and Kaczorowski D 2015 *J. Alloys Compd.* **646** 291–7
[18] Bednarchuk O and Kaczorowski D 2015 *Acta Phys. Pol.* A **127** 418–20
[19] Kakihana M *et al* 2017 *J. Alloys Compd.* **694** 439–51
[20] Céolin D *et al* 2013 *J. Electron Spectrosc. Relat. Phenom.* **190** 188–92
[21] Rueff J-P *et al* 2015 *J. Synchrotron Radiat.* **22** 175–9
[22] Ablett J M *et al* 2019 *J. Synchrotron Radiat.* **26** 263–71
[23] Mao H K, Xu J and Bell P M 1986 *J. Geophys. Res.* **91** 4673–6
[24] Tanaka A and Jo T 1994 *J. Phys. Soc. Japan* **63** 2788–807
[25] Cowan R D 1968 *J. Opt. Soc. Am.* **58** 808–18
[26] Mizuguchi Y *et al* 2017 *Phys. Rev.* B **95** 064515
[27] Utsumi Y, Kasinathan D, Swatek P, Bednarchuk O, Kaczorowski D, Ablett J M and Rueff J-P 2018 *Phys. Rev.* B **97** 115155
[28] Abd-Elmeguid M M, Sauer C and Zinn W 1985 *Phys. Rev. Lett.* **55** 2467–70

[29] Mitsuda A, Kishaba E, Fujimoto T, Oyama K, Wada H, Mizumaki M, Kawamura N and Ishimatsu N 2018 *Phys.* B **536** 427–31
[30] Hesse H-J and Wortmann G 1994 *Hyperfine Interact.* **93** 1499–504
[31] Matsubayashi K *et al* 2011 *Phys. Rev.* B **84** 024502
[32] Giannozzi P *et al* 2017 *J. Phys.: Condens. Matter* **29** 465901
[33] Dal Corso A 2014 *Comput. Mater. Sci.* **95** 337–50
[34] Perdew J P, Ruzsinszky A, Csonka G I, Vydrov O A, Scuseria G E, Constantin L A, Zhou X and Burke K 2008 *Phys. Rev. Lett.* **100** 136406
[35] Perdew J P, Ruzsinszky A, Csonka G I, Vydrov O A, Scuseria G E, Constantin L A, Zhou X and Burke K 2009 *Phys. Rev. Lett.* **102** 039902
[36] Marzari N, Vanderbilt D, De Vita A and Payne M C 1999 *Phys. Rev. Lett.* **82** 3296–9
[37] Cococcioni M and de Gironcoli S 2005 *Phys. Rev.* B **71** 035105
[38] Löwdin P-O 1955 *Phys. Rev.* **97** 1474–89
[39] Anisimov V I, Zaanen J and Andersen O K 1991 *Phys. Rev.* B **44** 943–54
[40] Anisimov V I, Solovyev I V, Korotin M A, Czyżyk M T and Sawatzky G A 1993 *Phys. Rev.* B **48** 16929–34
[41] Liechtenstein A I, Anisimov V I and Zaanen J 1995 *Phys. Rev.* B **52** R5467–70
[42] Kulik H J, Cococcioni M, Scherlis D A and Marzari N 2006 *Phys. Rev. Lett.* **97** 103001
[43] Timrov I, Marzari N and Cococcioni M 2018 *Phys. Rev.* B **98** 085127
[44] Bi W *et al* 2012 *Phys. Rev.* B **85** 205134
[45] Debessai M, Matsuoka T, Hamlin J J, Schilling J S and Shimizu K 2009 *Phys. Rev. Lett.* **102** 197002
[46] Röhler J 1986 *Physica B+C* **144** 27–31
[47] Johansson B and Rosengren A 1975 *Phys. Rev.* B **11** 2836–57
[48] Bi W *et al* 2016 *Phys. Rev.* B **93** 184424
[49] Pi S T, Savrasov S Y and Pickett W E 2019 *Phys. Rev. Lett.* **122** 057201
[50] Kotani A, Kvashnina K O, Glatzel P, Parlebas J C and Schmerber G 2012 *Phys. Rev. Lett.* **108** 036403
[51] Yamaoka H *et al* 2006 *J. Phys. Soc. Japan* **75** 034702
[52] Ichiki K *et al* 2017 *Phys. Rev.* B **96** 045106